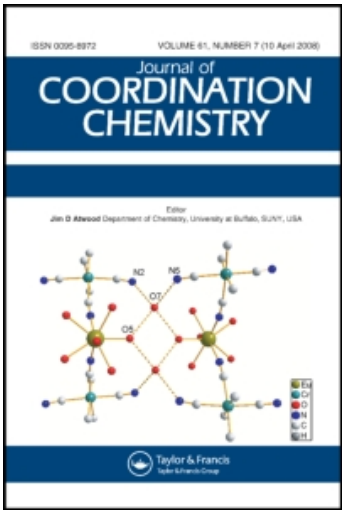

Journal of Coordination Chemistry
Publication details, including instructions for authors and subscription information:
http://www.informaworld.com/smpp/title~content=t713455674

Complex Formation Reactions of Divinyltin(IV) Complexes with Amino Acids, Peptides, Dicarboxylic acids and Related Compounds

Mahmoud M. A. Mohamed[a]
[a] Department of Chemistry Faculty of Education, Assuit University, Egypt

Online publication date: 15 September 2010

To cite this Article Mohamed, Mahmoud M. A.(2003) 'Complex Formation Reactions of Divinyltin(IV) Complexes with Amino Acids, Peptides, Dicarboxylic acids and Related Compounds', Journal of Coordination Chemistry, 56: 9, 745 — 759
To link to this Article: DOI: 10.1080/0095897031000110619
URL: http://dx.doi.org/10.1080/0095897031000110619

J. Coord. Chem., Vol. 56, No. 9, 15 June 2003, pp. 745–759

Taylor & Francis
Taylor & Francis Group

COMPLEX FORMATION REACTIONS OF DIVINYLTIN(IV) COMPLEXES WITH AMINO ACIDS, PEPTIDES, DICARBOXYLIC ACIDS AND RELATED COMPOUNDS

MAHMOUD M.A. MOHAMED*

Department of Chemistry, Faculty of Education, Assuit University, New Valley, Egypt

(Received 22 May 2002; Revised 6 August 2002; In final form 5 February 2003)

Complex formation equilibria of divinyltin(IV) with amino acids, peptides, and dicarboxylic acids have been investigated. Stoichiometry and stability constants for the complexes formed were determined at 25°C and ionic strength 0.1 M $NaNO_3$. The results showed the formation of ML, MLH, and ML_2 (organotin : ligand : hydrogen) complexes with amino acids. Peptides form ML complexes and the corresponding deprotonated amide species MLH_{-1}. In the latter species the binding with divinyltin(IV) occurs through the terminal amino group, carboxylate oxygen, and the amide nitrogen atoms (CO_2^-, N_{amide}^-, NH_2). The results showed the formation of ML and ML_2 complexes with dicarboxylic acids. The concentration distribution of the complexes in solution was evaluated. The bonding sites of the divinyltin(IV) complex in solid state with oxalic acid was investigated by means of elemental analyses, FTIR, and mass spectra. Non-isothermal decomposition of the above complex has been studied and the result was statistically analyzed. The main steps were identified for the thermal decomposition reaction and each step proved to be a first order reaction. The kinetic parameters E_a and A were calculated for each step in the reaction. The thermodynamic functions H, G, and S^* were calculated for each step of the reaction.

Keywords: Equilibrium studies; Thermal analysis (TGA & DTA); FTIR; Divinyltin(IV) complexes; Amino acid; Peptide; Dicarboxylic acids

INTRODUCTION

Organotin(IV) compounds R_nSnX_{4-n} exhibit a variety of pharmaceutical applications depending on the number n, on the type of organic groups R bound to tin and on the ligand X^-. Organotin compounds have been studied as possible candidates for antitumor activity, chemotherapy leishmaniasis and helminthes, and parasitic infection of the skin [1,2].

It has been established that the $R_2Sn(IV)^{2+}$ compounds which exhibit maximum antitumor activity combined with low mammalian toxicity are adducts of the type $R_2SnX_2L_2$ (X = halogen, pseudohalogen; L = O- or N-donor ligand) [3–9]. Therefore, a relationship between the stability of the organotin compound and their antitumor activity is indicated. Improving the bioavailability of the organotin(IV) cations by

*E-mail: mmhm80@hotmail.com

ISSN 0095-8972 print: ISSN 1029-0389 online © 2003 Taylor & Francis Ltd
DOI: 10.1080/0095897031000110619

formation of water soluble complexes [10] or by inclusion into β-cyclodextrin [11] have been attempted. During the last two decades, the interest of many scientists in the chemistry of methyl, ethyl, and butyl derivatives of tin(IV) has risen, but no study is available on the solution chemistry of divinyltin(IV).

Equilibrium study of organotin(IV) complexes with amino acids, peptides, dicarboxylic acids, or DNA constituents might provide further information on their antitumor and cytotoxic activity. In conjunction with our research project directed to study the solution chemistry of organotin(IV) complexes of ligands of biochemical significance [12–16], the present investigation aims to characterize divinyltin(IV) complex formation equilibria with some selected amino acids, peptides, and dicarboxylic acids. $[(Vinyl)_2Sn\text{-}(Oxa)] \cdot 3H_2O$ (Oxa = oxalic acid) was isolated and characterized by elemental analysis, FTIR, mass spectra, and thermal analysis (TGA and DTA).

EXPERIMENTAL

Materials and Reagents

Divinyltin(IV) dichloride was purchased from Strem Chemicals Co. The ligands (L) used were glycine, alanine, proline, valine, β-phenylalanine, isoleucine, threonine, methionine, aspartic acid, glutamic acid, histidine, histamine · 2HCl, lysine · HCl, ornithine · HCl, mercaptoethylamine · HCl, cysteine, glycinamide · HCl, glycylglycine, glycylalanine, glycylleucine, oxalic acid, cyclobutane dicarboxylic acid, malonic acid, succinic acid, adipic acid, and en · 2HCl. These materials were supplied by Fluka Chem. Co. Carbonate-free sodium hydroxide stock solutions were prepared by diluting the contents of BDH concentrated volumetric solution vials. These solutions were systematically checked by titration against potassium hydrogen phthalate. All solutions were prepared in deionized water.

SYNTHESIS

$[(Vinyl)_2Sn\text{-}(Oxa)] \cdot 3H_2O$ (where Oxa = oxalic acid) was prepared by dissolving oxalic acid (180 mg, 1 mmol) in a few mLs of water solution, and adding it dropwise to a stirred solution of divinyltin(IV) dichloride (486 mg, 1 mmol) in 10 mL water solution without heating. A white precipitate formed and the mixture was stirred for a further 2 h at 25°C. The precipitate was filtered off and washed sequentially with water and diethylether. Yield (95%) of white powder. Anal. Calcd. for $[C_6H_6O_4Sn] \cdot 3H_2O$, C: 22.9; H: 1.9; Sn: 42.8. Found C: 22.7; H: 2.0; Sn: 43.0.

Apparatus

The pH titrations were performed on a Metrohm 686 titroprocessor equipped with a 665 Dosmat. The titroprocessor was calibrated with standard buffer solutions prepared according to NBS specification [17].

The pH meter readings were converted into hydrogen ion concentration by titrating a standard acid solution (0.01), the ionic strength of which was adjusted to 0.1 M with $NaNO_3$, with standard base (0.1 M) at 25°C. The p(H) is plotted against p[H]. The relationship $p(H) - p[H] = 0.05$ was observed. The pK_w was calculated as described previously [16].

IR spectra were measured on an 80486-PC FTIR Shimadzu spectrophotometer using KBr pellets. Thermal analysis (TGA and DTA) were performed in nitrogen atmosphere with a TGA-50 and DTA-50 Shimadzu thermogravimetric analyzer. About 10 mg of the sample were used in a platinum cell with a 20 mL/min flow rate of nitrogen and a heating rate of 10 deg/min. Mass spectra were measured on a Shimadzu GC-Mass spectrometer.

Procedure and Measuring Techniques

The protonation constants of the ligands were determined by titrating 40 mL of ligand solution (2.5 mM). The hydrolysis constants of divinyltin(IV) were determined by titrating 40 mL of divinyltin(IV) solution with concentrations 2.5 mM and 1.25 mM. The formation constants of divinyltin(IV) complexes were determined by titrating 40 mL of solution containing the ligand (2.5 mM) and divinyltin(IV) with concentrations 1.25 mM and 0.625 mM. The ionic strength was adjusted to 0.1 M by $NaNO_3$. The titrations were performed in a special vessel described previously [18] at 25°C in a purified N_2 atmosphere.

The species formed in the systems studied were characterized by the general equilibrium process (1), while the formation constants for these generalized species are given in Eq. (2).

$$pM + qL + rH \rightleftharpoons [M_pL_qH_r] \tag{1}$$

$$\beta_{pqr} = \frac{[M_pL_qH_r]}{[\mathbf{M}]^p[L]^q[H]^r} \tag{2}$$

The calculations were performed using the computer program MINIQUAD-75 [19] loaded on an IBM-486 computer. The stoichiometries and stability constants of the complexes formed were determined by trying various composition models for the system studied. The model selected gave the best statistical fit and was chemically consistent with the titration data without giving any systematic drifts in the magnitudes of various residuals, as described elsewhere [19]. The model was tested by comparing the experimental titration data points and the theoretical curve calculated from the values of acid dissociation constant of the ligand and formation constants of the corresponding complexes. Table I lists the stability constants together with their standard deviations and the sum of the square of residuals as obtained from the program MINIQUAD-75. Concentration distribution diagrams were obtained using the program SPECIES [20].

TABLE I Formation constants of $M_pL_qH_r$ species

System	*p*	*q*	*r*[a]	logβ[b]	*S*[c]
$(vinyl)_2Sn(IV)$	1	0	−1	−2.93(0.00)	6.5E-9
	1	0	−2	−7.89(0.01)	
	1	0	−3	−17.76(0.01)	
	1	0	−4	−29.03(0.01)	
	2	0	−2	−3.08(0.01)	
	2	0	−3	−7.98(0.02)	

(*continued*)

TABLE I Continued

System	*p*	*q*	r^a	$\log\beta^b$	S^c
Glycine	0	1	1	9.60(0.01)	1.5E-7
	0	1	2	11.93(0.02)	
	1	1	0	10.65(0.05)	2.7E-7
	1	2	0	19.38(0.07)	
	1	1	1	13.96(0.08)	
Alanine	0	1	1	9.69(0.01)	9.3E-8
	0	1	2	11.89(0.02)	
	1	1	0	9.70(0.06)	3.1E-8
	1	2	0	17.44(0.06)	
	1	1	1	13.07(0.04)	
Proline	0	1	1	10.52(0.01)	4.4E-8
	0	1	2	12.03(0.04)	
	1	1	0	10.59(0.03)	6.4E-9
	1	2	0	19.19(0.04)	
	1	1	1	13.85(0.02)	
Valine	0	1	1	9.57(0.01)	10.0E-8
	0	1	2	11.71(0.02)	
	1	1	0	9.46(0.04)	1.7E-8
	1	2	0	16.95(0.05)	
	1	1	1	12.83(0.03)	
β-Phenylalanine	0	1	1	9.12(0.01)	8.0E-8
	0	1	2	11.01(0.03)	
	1	1	0	10.40(0.04)	4.9E-9
	1	2	0	18.65(0.07)	
	1	1	1	13.66(0.04)	
Methionine	0	1	1	9.10(0.01)	9.0E-8
	0	1	2	11.09(0.03)	
	1	1	0	10.12(0.01)	7.3E-9
	1	2	0	17.95(0.02)	
	1	1	1	13.26(0.01)	
Serine	0	1	1	9.14(0.01)	1.7E-8
	0	1	2	11.40(0.01)	
	1	1	0	9.88(0.01)	8.6E-8
	1	2	0	16.50(0.04)	
	1	1	1	13.39(0.06)	
	1	1	−1	3.48(0.07)	
Histidine	0	1	1	9.60(0.01)	2.6E-7
	0	1	2	15.92(0.03)	
	0	1	3	18.15(0.06)	
	1	1	0	11.52(0.08)	3.7E-8
	1	2	0	18.66(0.07)	
	1	1	1	16.51(0.06)	
Histamine	0	1	1	9.88(0.01)	2.4E-8
	0	1	2	15.97(0.01)	
	1	1	0	12.75(0.04)	4.3E-8
	1	2	0	19.57(0.07)	
	1	1	1	17.86(0.04)	
en · 2HCl	0	1	1	10.35(0.00)	4.5E-9
	0	1	2	17.83(0.01)	
	1	1	0	14.02(0.06)	7.7E-8
	1	2	0	20.24(0.09)	
	1	1	1	19.26(0.08)	
Ornithine	0	1	1	10.66(0.00)	7.7E-9
	0	1	2	19.51(0.01)	
	0	1	3	21.45(0.01)	
	1	1	0	14.21(0.05)	1.7E-8
	1	2	0	19.45(0.03)	
	1	1	1	19.26(0.05)	
	1	1	2	22.58(0.04)	

(*continued*)

TABLE I Continued

System	*p*	*q*	*r*[a]	logβ[b]	*S*[c]
Lysine	0	1	1	10.93(0.00)	1.7E-8
	0	1	2	20.20(0.01)	
	0	1	3	22.53(0.01)	
	1	1	0	15.09(0.02)	1.5E-8
	1	2	0	20.04(0.02)	
	1	1	1	20.11(0.03)	
	1	1	2	23.37(0.03)	
Aspartic acid	0	1	1	9.76(0.00)	4.4E-9
	0	1	2	13.45(0.01)	
	0	1	3	15.24(0.01)	
	1	1	0	11.39(0.03)	2.4E–10
	1	2	0	19.39(0.04)	
	1	1	1	14.09(0.03)	
	1	1	2	17.30(0.03)	
Glutamic acid	0	1	1	9.42(0.01)	2.2E-8
	0	1	2	13.50(0.01)	
	0	1	3	15.34(0.02)	
	1	1	0	11.79(0.05)	7.2E-8
	1	2	0	19.76(0.07)	
	1	1	1	15.55(0.05)	
	1	1	2	18.75(0.05)	
Mercaptoethylamine	0	1	1	10.37(0.01)	3.7E-8
	0	1	2	18.64(0.02)	
	1	1	0	15.58(0.02)	4.2E-9
	1	2	0	19.58(0.06)	
	1	1	1	20.40(0.04)	
Cysteine	0	1	1	10.63(0.01)	4.7E-8
	0	1	2	19.18(0.02)	
	0	1	3	21.62(0.05)	
	1	1	0	18.88(0.05)	5.5E-8
	1	2	0	23.54(0.06)	
	1	1	1	23.76(0.08)	
1,1-Cyclobutane dicarboxylic acid	0	1	1	5.42(0.00)	1.9E-8
	0	1	2	8.06(0.01)	
	1	1	0	7.44(0.02)	3.6E-9
	1	2	0	12.23(0.02)	
Oxalic acid	0	1	1	3.83(0.00)	1.3E-9
	0	1	2	5.66(0.01)	
	1	1	0	8.41(0.09)	8.0E-8
Malonic acid	0	1	1	5.30(0.00)	2.0E-9
	0	1	2	7.86(0.01)	
	1	1	0	6.71(0.04)	7.7E-9
	1	2	0	12.10(0.03)	
Succinic acid	0	1	1	5.27(0.00)	5.3E-10
	0	1	2	9.26(0.00)	
	1	1	0	6.22(0.03)	4.4E-9
	1	2	0	10.91(0.03)	
Adipic acid	0	1	1	5.11(0.00)	3.5E-9
	0	1	2	9.35(0.01)	
	1	1	0	6.13(0.04)	7.7E-9
	1	2	0	10.95(0.03)	
Glycinamide	0	1	1	7.50(0.01)	3.1E-8
	1	1	0	7.47(0.03)	1.8E-9
	1	1	−1	3.62(0.01)	
Glycylglycine	0	1	1	7.94(0.01)	2.5E-8
	0	1	2	10.80(0.01)	1.1E-7
	1	1	0	8.32(0.04)	
	1	1	−1	3.26(0.04)	

(*continued*)

TABLE I Continued

System	*p*	*q*	*r*[a]	logβ[b]	*S*[c]
Glycylalanine	0	1	1	8.21(0.01)	4.4E-8
	0	1	2	11.01(0.02)	
	1	1	0	8.04(0.06)	2.9E-8
	1	1	−1	3.75(0.04)	
Glycylleucine	0	1	1	7.96(0.01)	2.0E-7
	0	1	2	11.28(0.02)	
	1	1	0	8.31(0.02)	9.8E-9
	1	1	−1	3.43(0.03)	

[a]*p*, *q*, and *r* are the stoichiometric coefficient corresponding to $(vinyl)_2Sn$, amino acid, dicarboxylic acid or peptide and H^+, respectively; [b]Standard deviations are given in parentheses; [c]Sum of square of residuals.

RESULTS AND DISCUSSION

Dissociation constants of the ligands were determined under the same experimental conditions of ionic strength and temperature as the divinyltin(IV) complexes. The results obtained are in good agreement with literature data [21].

Hydrolysis of the diorganotin(IV) cations form stable and water soluble mono- and polynuclear hydroxo species in the whole pH-range studied [22–29]. Since the hydroxide ion and the ligands are in competition for the metal ion, these species were always taken into consideration in the equilibrium systems. The hydrolysis of the divinyltin(IV) was characterized by fitting the potentiometric data to various acid-base models. The fitted model was found to be consistent with the formation of $M(OH)$, $M(OH)_2$, $M(OH)_3$, $M(OH)_4$, $[M_2(OH)_2]$, and $M_2(OH)_3$ species. Estimation of the concentration distribution of various species in solution provides a useful picture of organotin(IV) binding in the biological system. In all the species distributions, the concentration of the complex increases with increasing pH, thus making complex formation more favored in the physiological pH range. The concentration distribution diagram for the $(vinyl)_2Sn$–OH system is shown in Fig. 1. The concentration of the dihydroxo species reaches the maximum concentration of 99.4% at pH = 7.4. Thus under physiological conditions the $M(OH)_2$ is predominating.

Complex Formation Equilibria Involving Amino Acids

The potentiometric titration curve of divinyltin(IV) complex is lowered from the corresponding amino acid curve, Fig. 2. This corresponds to the formation of a complex species through release of hydrogen ion. The potentiometric data of the amino acid complexes were fitted with the model composed of the species ML, ML_2, and MLH. In addition to these, MLH_2 is formed for histidine, ornithine, lysine, aspartic acid, and glutamic acid. The formation of ML_2 complexes is consistent with the previous finding for dimethyltin(IV) complexes with amino acids [30].

The acid dissociation constants of the protonated complexes are calculated using Eq. (3).

$$\begin{aligned} pK_1^H &= \log \beta_{MLH} - \log \beta_{ML} \\ pK_2^H &= \log \beta_{MLH_2} - \log \beta_{MLH} \end{aligned} \tag{3}$$

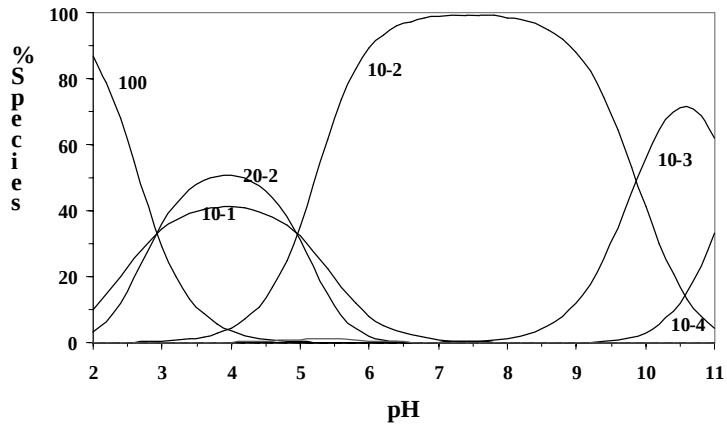

FIGURE 1 Species distribution of various species as a function of pH in the $(vinyl)_2Sn(IV)$ system (at concentration of 1.25 mmol/L).

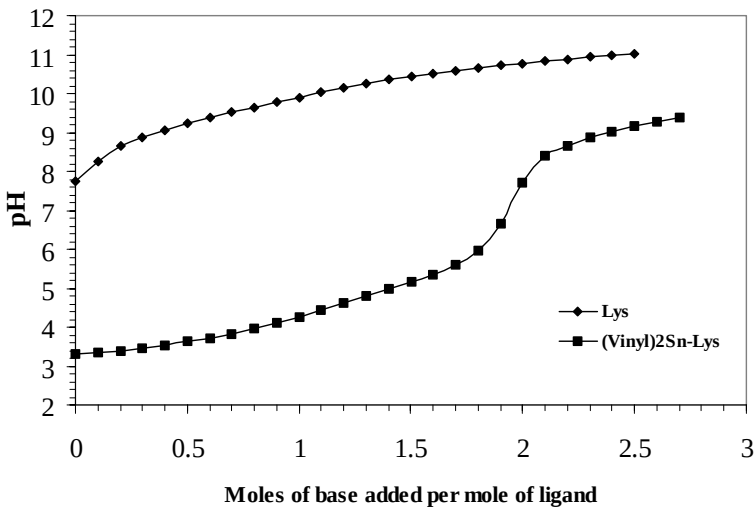

FIGURE 2 Potentiometric titration curves of $(vinyl)_2Sn$–lysine system.

Protonated MLH complexes are formed in acidic media. The pK_1^H of MLH species are in the range (3.14–3.51). The deprotonation of MLH (pK_1^H), corresponds to deprotonation of a metal-bound water (better described as MLH(OH) or to the metal ion-promoted deprotonation of the NH_3^+ group [31]. Similar pK_1^H values (difference $\sim$0.37), regardless of the α-amino acid indicate that the proton is dissociating from the same donor site. Deprotonation of a coordinated water in the dimethyltin(IV)-acetate species having the same set of donor atoms as the MLH species, this shows a pK value (4.14) higher than that of $(CH_3)_2Sn$(amino acid) [32,33]. These considerations suggest that deprotonation in MLH species is from an NH_3^+ group and not from coordinated water molecule. Consequently the amino acid is bidentate, coordinating by the amino and carboxylate group. This is not the only example of coordination of a nitrogen atom at a relatively low pH; it has been reported that in

the dimethyltin(IV)–IDA system (IDA = iminodiacetate) the nitrogen is involved in coordination at a pH value 2.5 [22,34].

Analysis of the titration results for $(vinyl)_2Sn(IV)$ with histidine, ornithine, lysine, aspartic acid, glutamic acid, or cysteine showed the formation of ML complexes with stability constants higher than those of the corresponding α-amino acids (CO_2^-, NH_2). This indicates that these amino acids bind through the amino, carboxylate, and terminal groups, e.g., histidine binds through (CO_2^-, NH_2, NH imidazole ring); ornithine and lysine bind through (CO_2^-, NH_2, terminal NH_2); aspartic acid and glutamic acid bind through (CO_2^-, NH_2, terminal CO_2^-); and cysteine binds through (CO_2^-, NH_2, S^-).

Serine has an extra binding center on the β-alcoholato-group. This group was reported [35] to participate in transition metal ion complex formation. The titration curve of the serine complex is lower than the curves of the other amino acid complexes in the region $2 \leq a \leq 3$, corresponding to the complete formation of its complex, Fig. 3. This may reveal that the β-alcoholato-group participates in complex formation. Also, the potentiometric data are better fit assuming formation of the complex species ML, MLH, ML_2, and MLH_{-1}. The pK_a value of the β-alcoholato-group incorporated in the $(vinyl)_2Sn$ complex ($\log\beta_{ML} - \log\beta_{MLH-1}$) is 6.40. This finding is supported by the observation that in basic solutions Cu(II) promotes ionization of the alcoholato-group of threonine with a pK_a value of 10.3 [36]. Participation of the thioether group [37] in the coordination of methionine with $(vinyl)_2Sn(IV)$ seems to be unfavored, because the stability constants of their complexes are in fair agreement with those of α-amino acids.

The species distribution for ornithine complex, taken as a representative, is given in Fig. 4. The ML complex attained the maximum formation degree (45.3% at pH *ca.* 7.0); the dihydroxo species $M(OH)_2$ attains a maximum concentration of 55.0% at pH = 8.0. This reveals that under physiological conditions the ML and $M(OH)_2$ predominate.

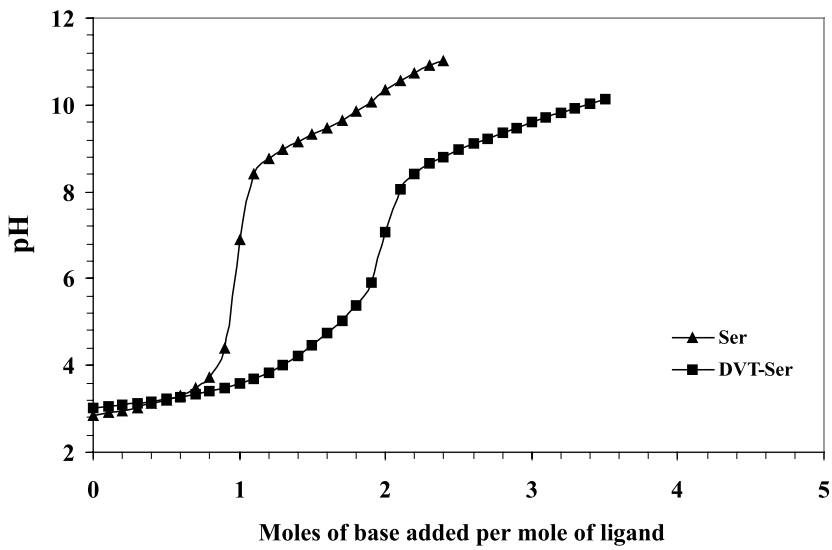

FIGURE 3 Potentiometric titration curve of $(vinyl)_2Sn(IV)$–serine system.

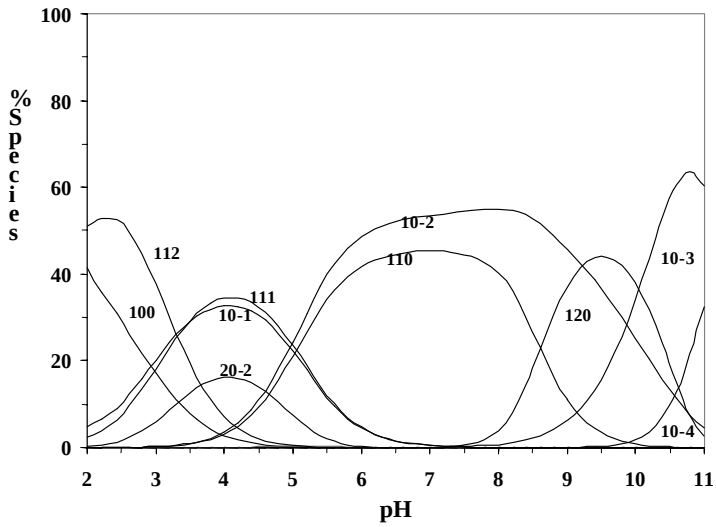

FIGURE 4 Species distribution of various species as a function of pH in the $(vinyl)_2Sn$–ornithine system (at concentration of 1.25 and 2.5 mmol/L, respectively).

Complex Formation Equilibria Involving Dicarboxylic Acids

In the $(vinyl)_2Sn(IV)$–dicarboxylic acid system computer analysis of the pH titration data showed the presence of the ML and ML_2 species. The results (Table I) show that the ML complex involving a five-membered chelate ring as in oxalic acid has the highest stability constant. The ML complex involving six-membered chelate rings as in cyclobutane dicarboxylic acid and malonic acid have higher stability constants than those of seven-membered chelated rings as in succinic acid, and eight-membered chelated rings as in adipic acid. This may be explained on the premise that five-membered rings are more energetically favored than the six and the six-membered rings are more favored than seven- and eight-membered rings. It is interesting to note that cyclobutane dicarboxylic acid has a higher stability constant than malonic acid. This may be due to hydrophobic contact between the cyclobutane ring of CBDCA and the vinyl group of $(vinyl)_2Sn(IV)$, supported by molecular models. A similar observation was found in the reaction of carboplatin and guanosine 5′-monophosphate [38].

The species distribution diagram of CBDCA, as a representative (Fig. 5) shows that the deprotonated complex ML_2 prevails with formation degree (85.4%) at $pH = 5.6$; the dihydroxo species $M(OH)_2$ attains a maximum concentration of 95.5% at $pH = 8.4$. The deprotonated species ML_2 and $M(OH)_2$ predominate in the physiological pH range.

Complex Formation Equilibria with Peptides

The potentiometric data of the $(vinyl)_2Sn$–peptide (L) systems were fitted to various models. The acceptable model was consistent with formation of complexes with stoichiometric coefficients ML and MLH_{-1}. Consequently the complex formation may be explained by the following equilibria.

$$(vinyl)_2Sn^{2+} + L^- \overset{K_1}{\rightleftharpoons} [(vinyl)_2Sn] - L^+ \tag{4}$$

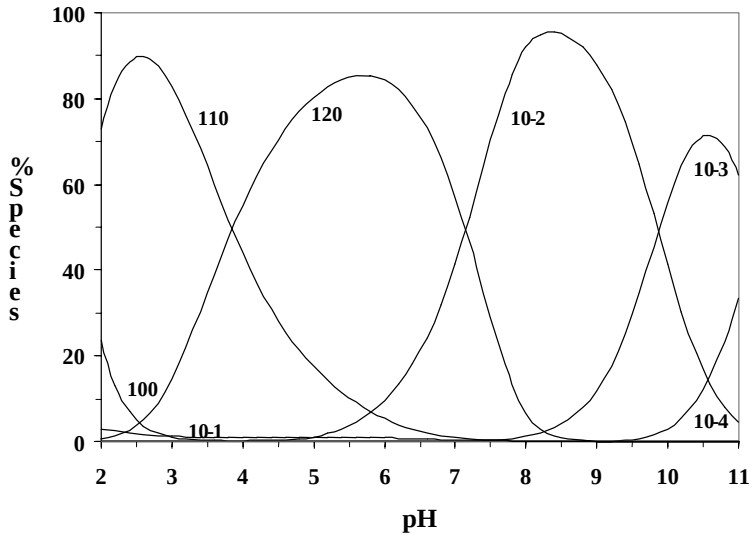

FIGURE 5 Species distribution of various species as a function of pH in the $(vinyl)_2Sn(IV)$–CBDCA system (at concentration of 1.25 and 2.5 mmol/L, respectively).

$$[(vinyl)_2Sn] - L^+ \overset{K_a}{\rightleftharpoons} [(vinyl)_2Sn] - LH_{-1} + H^+ \quad (5)$$

The pK_a of the ionized amide group is calculated by Eq. 5.

$$pK_a = \log\beta_{[(vinyl)_2Sn]-L^+} - \log\beta_{[(vinyl)_2Sn]-LH_{-1}}$$

The acid dissociation constant of the protonated complexes with peptides compare favorably with the acid dissociation constant of the protonated complexes of α-amino acids. This reveals that peptides bind to $(vinyl)_2Sn(IV)$ by a carboxylato group at low pH, while the amino group remains free. On increasing the pH, the amino and the amide groups undergo deprotonation and the complexes $[(vinyl)_2Sn(L)]$, (ML) and $[(vinyl)_2Sn(LH_{-1})]$, (MLH_{-1}) are formed. The binding in the MLH_{-1} complex involves the amino group and deprotonated amide-N atom. The pK_a values of the amide group, incorporated in the divinyltin(IV) complexes are in the range of (3.85–5.06).

Based on previous investigation on dipeptide–diorganotin(IV) complexes [12,22–24, 39], complex formation between divinyltin(IV) and glycylglycine results in a chelate involving the terminal amino moiety, carboxylate oxygen and the amide nitrogen atoms (CO_2^-, N^-_{amide}, NH_2).

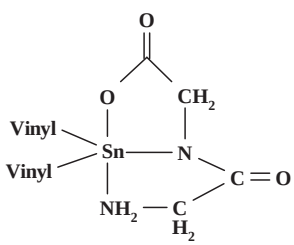

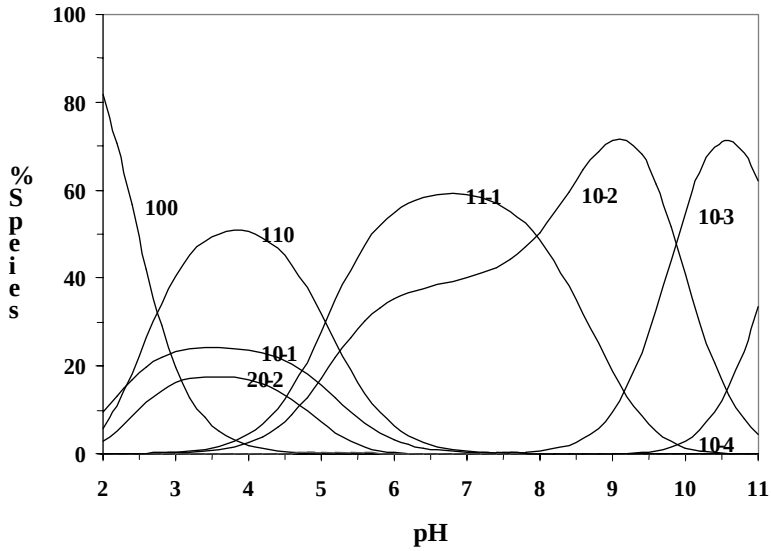

FIGURE 6 Species distribution of various species as a function of pH in the $(vinyl)_2Sn$–glycylglycine system (at concentration of 1.25 and 2.5 mmol/L, respectively).

The slight difference in the side chain of the peptide produces dramatic differences in their behavior toward the $(vinyl)_2Sn(IV)$ species. The slight difference in the side chain of the peptides has an effect on ionization of the amide group. The glycinamide complex has the smallest pK_a value. This is explained based on the assumption that the more bulky substituted group on the peptide hinders ionization of the amide group.

Distribution curves for divinyltin(IV) complexes with glycylglycine are given in Fig. 6. The concentration distribution diagrams for all $(vinyl)_2Sn$–peptide systems in the present study show the same qualitative features namely a progressive increase of ML concentration with pH reaching a maximum of 50.9% at pH $\approx$ 3.8 on further increase of pH, the MLH_{-1} concentration increases accompanied by a corresponding decrease in the concentration of ML species. The MLH_{-1} concentration reaches a limiting value of 59.1% at pH $\approx$ 6.8.

IR and TG Analysis

The IR spectra of the $[(vinyl)_2Sn\text{-}(Oxa)] \cdot 3H_2O$ complex exhibit a strong band at 3417.6 cm^{-1} for coordinated water molecules. The carboxylate stretching bands υ_{as} appear at 1695.0 and 1620.1 cm^{-1} and υ_s appears as a strong band at 1396.4 cm^{-1}. The Sn–O band appears at 617 cm^{-1}, while Sn–C bands appear at 578 (υ_{as}) and 509 cm^{-1} (υ_s) [40,41]. The mass spectral fragmentation of the $[(vinyl)_2Sn\text{-}(Oxa)] \cdot 3H_2O$ complex displays prominent peaks corresponding to the mononuclear parent ligand and tin(IV) ions, which may be discussed in terms of the valence change concept for rationalizing the major fragmentation pathways. The major fragmentation of $[(vinyl)_2Sn\text{-}(Oxa)] \cdot 3H_2O$ shows peaks at $m/z = 36$, 145, 155, 173, 206, and 315.

Figure 7(a) shows the TGA and DrTGA curves of $[(vinyl)_2Sn\text{-}(Oxa)] \cdot 3H_2O$ at a heating rate of 10°C. Details of the thermal decomposition are clear from the

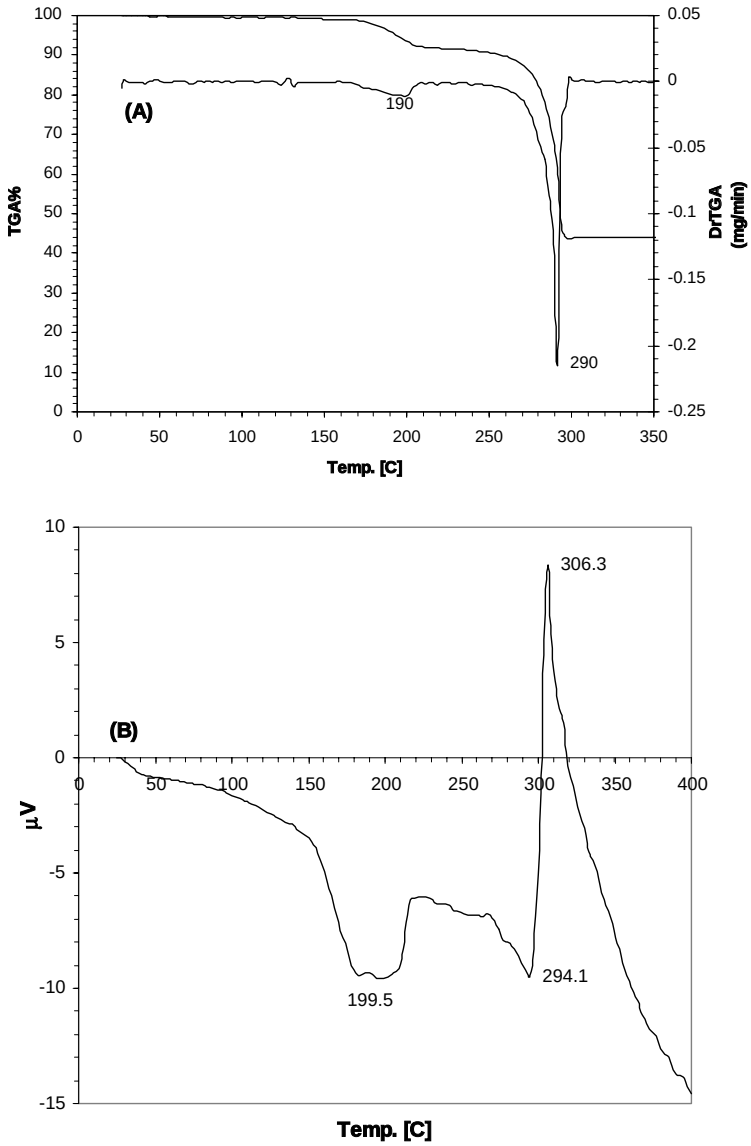

FIGURE 7 (a) TGA and DrTGA curves of $[(vinyl)_2Sn\text{-}(Oxa)]\cdot 3H_2O$ complex at a rate of heating of 10 deg/min. (b) Differential thermal analysis (DTA) curve for $[(vinyl)_2Sn\text{–}(Oxa)]\cdot 3H_2O$ complex at a rate of heating of 10 deg/min.

DrTGA curve given in the same figure, while Fig. 7(b) shows the differential thermal analysis (DTA) diagram. Table II, presents the results of the thermal investigations. Thermal decomposition of $[(vinyl)_2Sn\text{-}(Oxa)]\cdot 3H_2O$ can be characterized as a two-step reaction. The first step is the release of two water molecules at 190°C. Differential thermal analysis (DTA) showed an endothermic peak at 199.5°C which corresponds to the water loss. This step was confirmed by FTIR showing the same peaks of the starting complex. The second step corresponds to release of the ligand fragments leaving tin oxide. The release is accompanied by an endothermic peak at 294.1°C,

TABLE II Percentage mass loss accompanying the two decomposition stages of the complex

Complex	*Stage*	*Mass loss %*	
		Found	*Calc.*
$[(vinyl)_2Sn\text{-}(Oxa)]\cdot 3H_2O$	I	11.2	11.4
	II	45.8	45.8
	M%	43.0	42.8

then exothermic decomposition of the ligand in a very narrow temperature range between 294 and 320°C. The activation parameters (E and S^*) are 95.85 kJ/mol and -74.4 J/mol K (for the first step) and 426.12 kJ/mol and 509.5 J/mol K (for the second step). The positive value for S^* of the second step indicates that the reaction releases CO_2 and ethylene. Stable oxide [SnO_2 in air and a mixture of SnO and SnO_2 under N_2 (98%)] is the final product, which was confirmed by X-ray diffraction patterns and FTIR spectra [42,43].

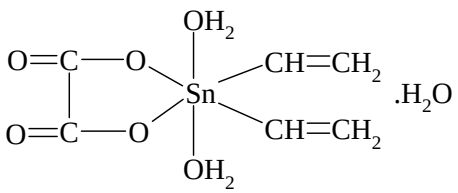

Analysis of the nonisothermal decomposition of the $[(vinyl)_2Sn\text{-}(Oxa)]\cdot 3H_2O$ complex is carried out according to Coats–Redfern [44]. The reaction order was estimated. The following equation was applied to fit the obtained thermal decomposition data:

$$\int_0^{\alpha} d\alpha(1-\alpha)^n = A/\varphi \int_0^{T} \exp(-E_a/RT)\, dt, \tag{6}$$

where α is the reaction fraction decomposed, φ is the heating rate, T is the absolute temperature at time t, n is the order of reaction, R is the gas constant in $J\,mol^{-1}\,K^{-1}$ and E_a is the activation energy in $Jmol^{-1}$.

The term $d\alpha(1-\alpha)^n$ has two different solutions, $1-(1-\alpha)^{1-n}/1-n$ for $n \neq 1$ and $-\log(1-\alpha)$ for $n=1$.

The right hand side in Eq. (3) has the solution

$$\frac{ART^2}{\varphi E_a}\left(\frac{1-2RT}{E_a}\right)\exp(-E_a/RT)$$

Taking the logarithm for $n \neq 1$, we get

$$\log\left(\frac{1-(1-\alpha)^{1-n}}{T^2(1-n)}\right) = \log\left(\frac{AR}{\varphi E_a}\frac{(1-2RT)}{E_a}\right) - \frac{E_a}{2.303RT}$$

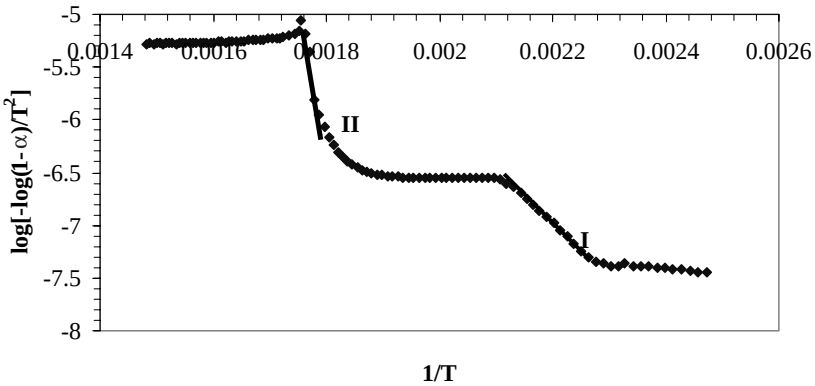

FIGURE 8 Plot $\log[-\log(1-\alpha)]/T^2$ *vs* $1/T$ of the $[(vinyl)_2Sn\text{-}(Oxa)]\cdot 3H_2O$ complex.

TABLE III Kinetic parameters for the nonisothermal decomposition of the $[(vinyl)_2Sn\text{-}(Oxa)]\cdot 3H_2O$ complex

Range °C	T_i[a] °C	*E* (KJ/mol)	*A* (s^{-1})	*S** (J/molK)	*G* (KJ/mol)	*H* (KJ/mol)
160–200	190	95.85	1.25×10^9	−74.4	130.3	92.0
280–300	290	426.12	3.96×10^{39}	509.5	135.3	421.4

[a]The peak temperature from the DTG curve.

The term $\log(AR/\varphi E_a)((1-2RT)/E_a)$ is almost constant. Plotting $\log[-\log(1-\alpha)/T^2]$ *vs* $1/T$, assuming a first order reaction, reveals linear relations for the different steps of decomposition (see Fig. 8). The Coats–Redfern equation has been applied to each step separately and the results were statistically analyzed (correlation coefficient of 0.980–0.998). From the slopes and intercepts of these lines the preexponential factor, A, and the activation, E_a, are calculated.

The entropies of activation S^* were calculated using Eq. (7) [45].

$$S^* = 2.303R \log Ah/kT_i \tag{7}$$

where h and k stand for the Planck and Boltzmann constants, respectively, and T_i is the peak temperature from the DTG curve. The free energy of activation G and the enthalpy of activation H were calculated using Eqs. (8) and (9), respectively.

$$G = E - T_i S \tag{8}$$

$$H \approx E - RT_i \tag{9}$$

The values of the thermodynamic parameters of activation are given in Table III.

Acknowledgment

The authors are indebted to Prof. Dr. M.M. Shoukry for his help and interest.

References

[1] W. Peters, E.R. Trotter and B.L. Robinson, *Ann. Trop. Med. Parasitol.* **74**, 321 (1980).
[2] L. Pellerito and L. Nagy, *Coord. Chem. Rev.* **224**, 111 (2002).
[3] N.F. Cardinelli (Ed.), *Tin as a Vital Nutrient* (CRC Press, Boca Raton, FL, 1985).
[4] A. Saxena and J.P. Tandon, *Cancer Lett.* **19**, 73 (1988).
[5] G. Atassi, *Rev. Si Ge Sn Ob Comp.* **8**, 821 (1985).
[6] A.K. Saxena, *Appl. Organomet. Chem.* **1**, 39 (1987).
[7] S.J. Blunden, P.A. Cusack and R. Hill, The Industrial Use of Tin Compounds (Royal Society of Chemistry, London, 1985).
[8] A.H. Penninks, M. Bol-Schoenmakers and W. Seinen, Cellular interactions of organotin compounds in relation to their antitumor activity. In: M. Gielen (Ed.), Tin-Based Antitumor Drugs, NATO ASI Series, Vol. H37 (Springer Verlag, Berlin 1990), p. 169.
[9] M. Gielen, R. Willem, T. Mancills, J. Ramharter and E. Joosen, In: J.J. Zuckerman (Ed.), Tin and Malignant Cell Growth (CRC Press, Cleveland, 1988).
[10] M. Gielen, In: N.F. Cardinelli (Ed.), Tin as a Vital Nutrient (CRC Press, Boca Raton, FL, 1985).
[11] J. Szejtli, Cyclodextrins and Their Inclusion Complexes (Akadémiai Kiadó, Budapest, 1982).
[12] M.M. Shoukry and M.M.A. Mohamed, *Main Group Met. Chem.* **20**, 281 (1997).
[13] M.M. Shoukry and M.M.H. Mohamed, *J. Coord. Chem.* **43**, 217 (1998).
[14] M.M. Shoukry, E.M. Khairy and M.M.A. Mohamed, *Talanta* **44**, 1149 (1997).
[15] A.A. Al-Najjar, M.R. Shehata, M.M.A. Mohamed and M.M. Shoukry, *Main Group Met. Chem.* **22**, 253 (1999).
[16] M.M.A. Mohamed, M.R. Shehata and M.M. Shoukry, *J. Coord. Chem.* **53**, 125 (2001).
[17] R.G. Bates, Determination of pH-Theory and Practice, 2nd Edn. (Wiley, New York, 1975).
[18] M.M. Shoukry, W.M. Hosny and M.M. Khalil, *Transition Met. Chem.* **20**, 252 (1995).
[19] P. Gans, A. Sabatini and A. Vacca, *Inorg. Chem. Acta* **18**, 237 (1976).
[20] L. Pettit, Personal Communication (University of Leeds).
[21] M.M. Shoukry, E.M. Khairy and R.G. Khalil, *Transition Met. Chem.* **22**, 465 (1997).
[22] G. Arena, R. Calì, A. Contino, A. Musumeci, S. Musumeci and R. Purrello, *Inorg. Chim. Acta*, **237**, 187 (1995).
[23] P. Surdy, P. Rubini, N. Buzás, B. Henry, L. Pellerito, T. Gajda, *Inorg. Chem.* **38**, 346 (1999).
[24] N. Buzás, T. Gajda, L. Nagy, E. Kuzmann, A. Vertes, K. Burger, *Inorg. Chim. Acta* **274**, 167 (1998).
[25] T. Natsume, S. Aizawa, K. Hatano and S. Funahshi, *J. Chem. Soc. Dalton Trans.* 2749 (1994).
[26] B. Noszal, V. Scheller-Krattiger and R. B. Martin, *J. Am. Chem Soc.*, **104**, 1078 (1982).
[27] C. De Stefano, C. Foti, A. Giaanguzza, M. Martino, L. Pellerito and S. Sammartano *J. Chem. Eng. Data*, **41**, 511 (1998).
[28] M.M.A. Mohamed and M.M. Shoukry, *Chem. Pharm. Bull.* **49**, 253 (2001).
[29] O. Al-Flaijj, M.R. Shehata, M.M.A. Mohamed and M. M. Shoukry, *Monatsh. Für Chem.* **132**, 349 (2001).
[30] M.M. Shoukry, *Talanta* **43**, 177 (1996).
[31] B. Gyurcsik, N. Buzás, T. Gajda, L. Nagy, E. Kuzmann, A. Vértes and K. Burger, Z. Naturforsch. **50**, 515 (1995).
[32] G. Arena, A. Gianguzza, L. Pellerito, R. Rurrello and E. Rizzarelli, *J. Chem. Soc. Dalton Trans.* 2603 (1990).
[33] G. Arena, A. Gianguzza, L. Pellerito, R. Rurrello and E. Rizzarelli, *J. Chem. Soc. Dalton Trans.* 773 (1989).
[34] V. Cucinotta, A. Gianguzza, G. Maccarrone, L. Pellerito, R. Purrello and E. Rizzarelli, *J. Chem. Soc. Dalton Trans.* 2299 (1992).
[35] M.L. Lim, *Inorg. Chem.* **20**, 1377 (1981).
[36] P. Grenouillet, R.B. Martin, A. Rossi and M. Ptak, *Biochim. Biophys. Acta* **322**, 185 (1973).
[37] U. Frey, J.D. Ranford and P.J. Sadler, *Inorg. Chem.* **32**, 1333 (1993).
[38] E.S. Freeman and B. Carroll, *J. Chem.* **62**, 394 (1958).
[39] A. Jancsó, B. Henry, P. Rubini, G. Vankó and T. Gajda, *J. Chem. Soc. Dalton Trans.* 1941 (2000).
[40] N. Buzás, B. Gyurcsik, L. Nagy, Y. Zhang, L. Korecz and K. Burger, *Inorg. Chim. Acta* **218**, 65 (1994).
[41] G.B. Deacon and R.J. Phillips, *Coord. Chem. Rev.* **33**, 227 (1980).
[42] D. Fregona, Z. Guo and G. Faraglia, *J. Coord. Chem.* **28**, 73 (1993).
[43] Textbook "Powder Diffraction File", International Center for Diffraction Data, 1990, 1601, Parklane, Swarthmore, PA 19081-2389, USA.
[44] A.W. Coats and J.P. Redfern, *Nature* **201**, 68 (1964).
[45] S. Glasstone, A Textbook of Physical Chemistry, 2nd Edn. (Macmillan, Bombay, India, 1974).